A&A 589, A48 (2016)
DOI: 10.1051/0004-6361/201628199

Astronomy & Astrophysics

Optical microflaring on the nearby flare star binary UV Ceti

J. H. M. M. Schmitt[1], G. Kanbach[2], A. Rau[2], and H. Steinle[2]

[1] Hamburger Sternwarte, Gojenbergsweg 112, 21029 Hamburg, Germany
e-mail: jschmitt@hs.uni-hamburg.de
[2] Max-Planck-Institut für extraterrestrische Physik, 85748 Garching bei München, Gießenbachstraße 1, Germany

Received 27 January 2016 / Accepted 11 March 2016

ABSTRACT

We present extremely high time resolution observations of the visual flare star binary UV Cet obtained with the Optical Pulsar Timing Analyzer (OPTIMA) at the 1.3 m telescope at Skinakas Observatory (SKO) in Crete, Greece. OPTIMA is a fiber-fed optical instrument that uses Single Photon Avalanche Diodes to measure the arrival times of individual optical photons. The time resolution of the observations presented here was 4 μs, allowing to resolve the typical millisecond variability time scales associated with stellar flares. We report the detection of very short impulsive bursts in the blue band with well resolved rise and decay time scales of about 2 s. The overall energetics put these flares at the lower end of the known flare distribution of UV Cet.

Key words. stars: activity – stars: flare – stars: low-mass

1. Introduction

Solar and stellar flares are known to occur on vastly different time scales, ranging from a few seconds (Vilmer et al. 1994; Schmitt et al. 1993) and possibly below (Beskin et al. 1982) to more than a week (Kürster & Schmitt 1996). The primary energy release process of solar and stellar flares is – at least according to the prevailing paradigm – coronal, but a substantial amount of energy is (often) emitted at optical wavelengths. The response of the plasma, heated by particle beams and shock waves, depends sensitively on the mode of energy input and is in fact radiated over many regions of the electromagnetic spectrum.

Because of their low contrast white light flares are rather difficult to observe on the Sun. However, on stars with sufficiently low effective temperatures the photospheric response of a coronal energy release produces emissions that dominate the overall stellar output, even when confined to quite small portions of the stellar surface. Most researchers agree that in the flare process some particle acceleration does take place in the corona, causing the accelerated particles and/or plasma waves to move along the magnetic field lines before finally reaching and heating cooler atmospheric layers (Syratovskii & Shmeleva 1972; Brown 1973). The heated chromospheric and photospheric layers are quite dense and start radiating essentially instantaneously, thus serving as a proxy indicator for non-thermal particles. On somewhat longer time scales the heated chromospheric layers "evaporate", leading to a soft X-ray flare (Neupert 1978; Peres 2000).

If the optical emission were also non-thermal, the relevant time scales could be very short indeed. If, however, the emission is thermal, as most researchers would assume, the relevant time scales are the typical propagation time of a shock $\tau_{\rm sh}$, driven by the flare explosion into the photospheric layers, and the radiative cooling time scale $\tau_{\rm th}$, on which a heated parcel of gas looses its energy by radiation. The shock propagation time can be estimated from the expression $\tau_{\rm sh} \sim H/v_{\rm sh}$, with H denoting the scale height of the emission layer and $v_{\rm sh}$ the shock speed. A conservative estimate of $\tau_{\rm th}$ can be derived in the diffusion approximation (which of course need not apply in the photosphere and chromosphere) and one finds – apart from geometry factors (cf., discussion by Sánchez Almeida 2001) – $t_{\rm th} \approx \frac{C_{\rm V}}{16\kappa_{\rm R}\sigma T^3}$, where $C_{\rm V}$ denotes the specific heat at constant volume, $\kappa_{\rm R}$ the Rosseland mean opacity, σ the Boltzmann constant and T the temperature. With typical parameters computed for a stellar photosphere one finds cooling times on the order of a few seconds. If a scenario of non-thermal heating and thermal cooling is assumed, one would thus expect cooling times on the order of seconds and heating time scales which in principle could be very short, i.e., similar to the time scales of non-thermal solar X-ray or γ-ray bursts (Vilmer et al. 1994).

A thorough study of the photospheric heating (and cooling) processes during flares thus requires observations with very high time resolution. Yet only few investigations of flare stars have been carried out at extremely high time resolution at the level of, say, milliseconds or less. Since our OPTIMA instrument (for a description see Sect. 2) does provide this temporal resolution, we decided to carry out some preliminary flare star observations in the msec range and below.

Of course, other flares star studies with high time resolution have been carried out with various instruments. Robinson et al. (1995) used the High Speed Photometer aboard the *Hubble* Space Telescope to study CN Leo with high time resolution (0.01 s) for 2 h in the UV (around 2400 Å) and detected a number of events with "substantial variations sometimes occurring on time scales of less than 1 s". Tovmassian et al. (1997) used smaller ground based telescopes to study the flare stars EV Lac and V 577 Mon with a time resolution of 0.1 s in the U and B-band and argue that some of the reported events have durations of less than 1 s. Similarly, Zhilyaev et al. (1998) report ground-based UBV observations again of EV Lac with a time resolution of down to 0.05 s, with some events having widths below 1 s.

The most systematic efforts we are aware of in that respect are the studies undertaken at the 6 m Special Astrophysical Observatory (SAO) using the Multichannel Analysis of

Nanosecond Intensity Alterations (MANIA); a detailed description of this hardware has been presented by Beskin et al. (1982). As with our OPTIMA instrument, MANIA recorded individual photon arrival times with a time resolution of 300 nsec. Most of the MANIA observations were taken with a Johnson U filter, some with a B filter, however, due to data storage limitations at the time only the strongest flares could be recorded for subsequent analysis. Needless to say, data storage is not an issue any more.

The MANIA team published data on a number of nearby flare stars (Beskin et al. 1988), in particular on UV Cet, here we present OPTIMA data on the nearby (d = 2.62 pc) flare star binary UV Cet (=Gl 65 A+B). According to the SIMBAD data base, both components are spectral type dM5.5e, the brighter component has a visual magnitude of 12.57 mag with a $B - V$ color of 1.85 mag, while the B component with a visual magnitude of 12.7 mag is only a little fainter. Both components are dMe stars, both are known to be active, and both are known to produce flares. Both binary components have also been detected at X-ray (Audard et al. 2003) and radio wavelengths (Jackson et al. 1989), with the B component usually being the more active one. According to Geyer et al. (1988) the two components orbit each other in a rather eccentric orbit with a period of 25.52 yr; at the time of our observations the two stars were separated by a little under 2 arcsec at a position angle of 50°.

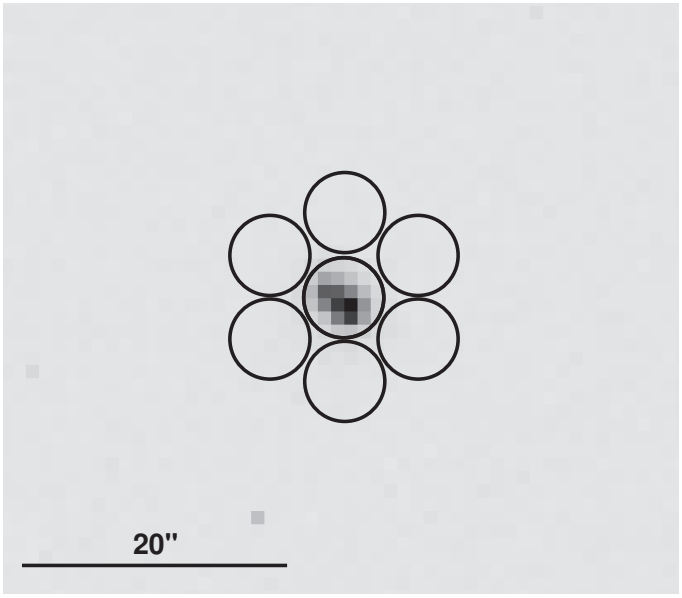

Fig. 1. Image of the UV Cet system taken with the OPTIMA field viewing CCD camera. The positions of the optical fibers are indicated relative to the location of the target.

2. Observations and data reduction

The observations reported in this paper were taken with the Optical Pulsar Timing Analyzer (OPTIMA) mounted at the 1.3 m telescope at Skinakas Observatory (SKO) in Crete, Greece in 2008. OPTIMA is a transportable visiting instrument that was operated at SKO for several weeks each year between 2006 and 2012. It records the arrival times of individual optical photons using eight single photon avalanche diodes (SPADs). Each diode is fed with by an optical fiber mounted in the telescopes optical plane on a slanted mirror. A central ("target", cf., Fig. 1) fiber is surrounded hexagonally by six outer fibers, while an eighth fiber observes the sky background a few arcmin away from the target.

The observations discussed here have been performed with a set of 300 μm diameter fibers corresponding to 6 arcsec on the sky; thus it is clear that the two components of UV Cet cannot be resolved by OPTIMA. The data acquisition system used in 2008 recorded all photons from the eight SPADs together with a time stamp accurate to 4 μs and synchronized with a GPS signal in absolute time. At this time resolution dead time effects become important at count rates above $\approx 10^5$ ct/s. The data were stored in a buffer, which, once full, was written to a hard drive. During this writing process no further data were recorded leading to an additional dead time of several seconds approximately every hour. In addition, to the photons recorded by the SPADs photons arriving outside the fibers are reflected on the slanted mirror and imaged with a CCD camera. Here, series of exposures with integration times of 10 s are obtained to monitor for variations in atmospheric transmission and seeing during an OPTIMA observation.

A typical OPTIMA observing sequence of a source starts with dark current measurements of the SPADs for about three minutes (cf., Fig. 3). Then the telescope is slewed towards a source-free position in the vicinity of the target for sky background measurements, again typically for a about three minutes. Afterwards the telescope is repositioned onto the target and the actual science data taking commences. At the end of the observations this sequence is reversed and another set of sky background and SPAD dark current measurements is taken.

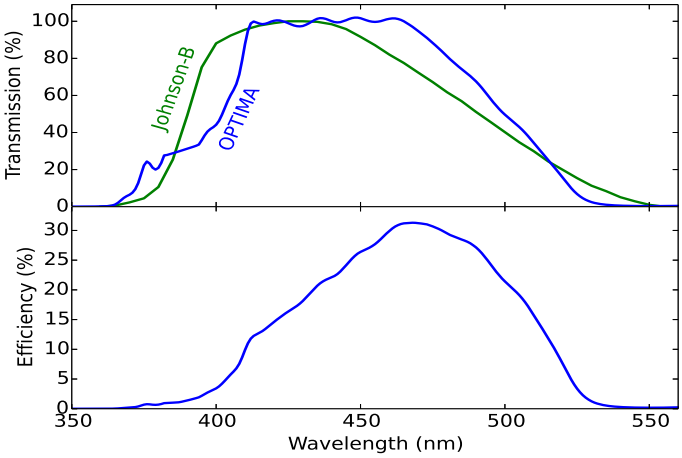

Fig. 2. *Top*: comparison of the transmission of blue filter used within OPTIMA and the standard Johnson B-band filter. *Bottom*: overall efficiency of OPTIMA with the blue filter taking into account the quantum efficiency of the single photon avalanche diodes.

A blue filter can be inserted into the light path of the fibers; the filter is transmissive in a relatively narrow wavelength range between 4000 Å and 4600 Å, while the quantum efficiency of the SPADs peaks at ≈7000 Å with very little transmission below 4000 Å. For the later analysis it is important to realize that this filter does not reproduce any of the standard color systems. However, its effective transmission curve resembles that of the standard B filter in the Johnson UBV system (see Fig. 2). The above summarizes the instrument as it was used for the UV Cet observations in 2008. More details can be found in Kanbach et al. (2008). Since then, OPTIMA has continuously evolved and its performance has been upgraded.

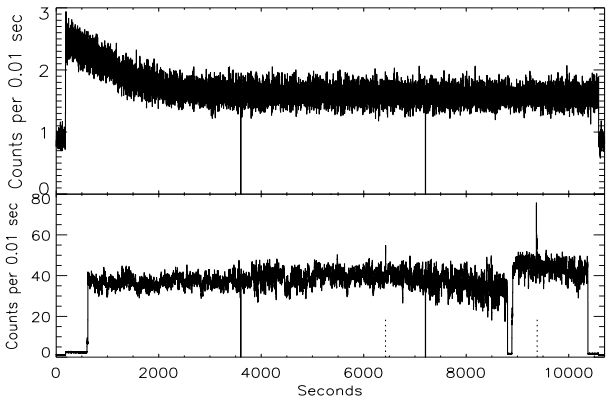

Fig. 3. OPTIMA light curve of UV Cet (*bottom panel*) and a nearby sky background position (*top panel*) taken on October 7th 2008. The flares of interest are indicated by the dotted lines; see text for more details.

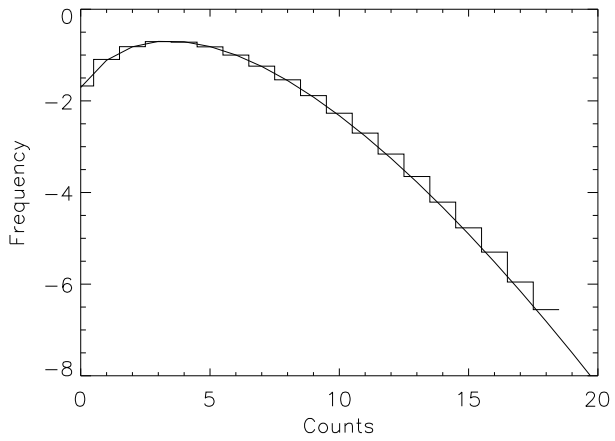

Fig. 4. Comparison of observed distribution of counts per millisecond (solid histogram) for the second hour of OPTIMA data of UV Cet with a Poisson distribution with the observed mean (solid curve).

3. Results

3.1. OPTIMA observations of UV Cet

During our 2008 OPTIMA observing campaign at SKO we observed the UV Cet binary system on October 6th and 7th for about 3 h each. Useful data with stable pointing were obtained for about 5000 s in the first night and 10 000 s in the second night.

Given the binary separation of below 2 arcsec and the OPTIMA fiber size of 6 arcsec, it is clear that the two binary components cannot be separated with the available instrumental setup as demonstrated in Fig. 1, where we show the hexagonal OPTIMA fibers as appearing on the sky. In order to give an impression of the quality of our OPTIMA data on UV Cet, we show in Fig. 3 the raw data (binned to a time resolution of 1 s) obtained in the central channel during the second night (bottom panel) as well as a background channel close to the target (top panel); note that the zero point of the time refers to UTC 21:02:34, Oct. 7, 2008. One recognizes very clearly the dark measurements at the beginning and at the end of the UV Cet run and, further, the sky background continuously decreased during the first 20 min of the observations (the Moon was setting at the time), however, its level amounts to less than 5% of the overall source signal.

The data drops at approximately 3600 s and 7200 s are caused by reading out of the full buffer when no new data can be stored as described above. The data drop near $T \approx 8800$ s is caused by a loss of pointing and subsequent reacquisition of the target.

An inspection of the data obtained in the other channels shows that these channels are dominated by background, however some leakage does occur as apparent from the data drop during the auto guider loss. However, that leakage is smaller than the additional background in these channels and we therefore refrain from adding channels. Since we are performing only relative photometry some losses through leakage are immaterial. In Fig. 3 two events are marked as flares at times of about 6450 s and 9370 s, which at frist are not very conspicuous but are actually significant short duration flares on UV Cet as we will show below.

3.2. Overall variability on short time scales

We first inspect our data for the properties of the event statistics. We specifically consider one hour of data without any instrumental interruptions and consider a data sampled with a cadence of 1 ms; the corresponding count histogram (constructed from 3.6×10^6 samples) together with a Poisson distribution with the same expectation value is shown in Fig. 4, which demonstrates that the the Poisson distribution does provide a good description of the data. We do, however, mention in passing that an inspection of the moments of the observed count distribution shows that its variance, skewness and kurtosis are somewhat larger than expected for a pure Poissonian distribution with the same mean, the values of kurtosis being about 8% larger. Obviously, the observed distribution has more outliers than a pure Poissonian case.

As we are interested in the source intrinsic variability on time scales of a few milliseconds all other potential contributions to the variability as well as to the uncertainties must be investigated. The scintillation phenomenon is well known to produce variability on these time scales of interest (Dravins et al. 1997). Scintillation, i.e., the "twinkling of stars", is caused by turbulence in the high atmosphere at altitudes of ten or more kilometers. Inhomogeneities in temperature and density lead to inhomogeneities in the refractive index, which cause random phase changes in a transmitted wave field of a celestial source. As a consequence, the wave field is distorted and the illumination on the ground will be inhomogeneous, too. A telescope with some given aperture will capture variable amounts of light. With increasing aperture one integrates over a larger number of atmospheric turbulence elements and therefore effectively depresses scintillation effects. According to theory the recorded scintillation intensity is expected to follow a log-normal distribution. This distribution is sampled in the observation as winds in the upper atmosphere transport the turbulent elements across the telescope aperture. On time scales sufficiently short the atmosphere is "frozen-in", since all light has traversed the same realisation of turbulent elements, and different samples are not statistically independent, leading to an autocorrelation of the recorded stellar signals.

We therefore checked the autocorrelation structure of our UV Cet data. In order to construct the autocorrelation function (ACF), we considered light curve chunks of 10 s each. For each of these intervals the ACF was computed for time lags of multiples of 1 ms and a mean ACF was computed. In Fig. 5 we plot the resulting mean ACF which is seen to indeed increase towards small time lags as expected from scintillation, however, the correlation effects are still relatively small. We carried out a similar analysis on the background channels and found no significant autocorrelation values on the relevant time scales.

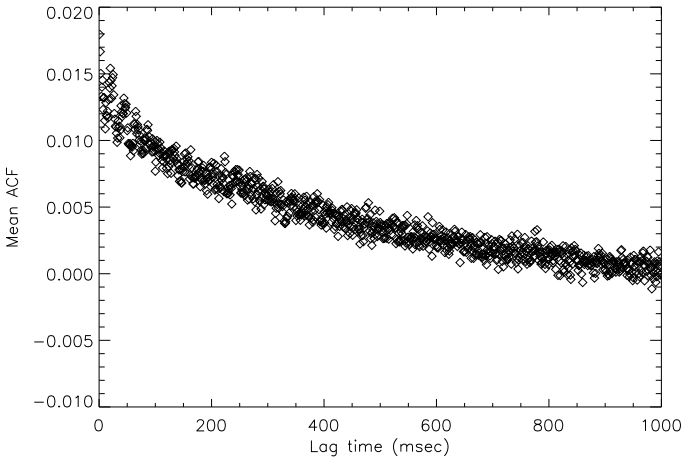

Fig. 5. Mean autocorrelation function ACF vs. lag (in ms) for the second hour of OPTIMA data of UV Cet. The sharp rise towards small lag times indicates the presence of scintillation effects, the slow decay indicates unaccounted fluctuations.

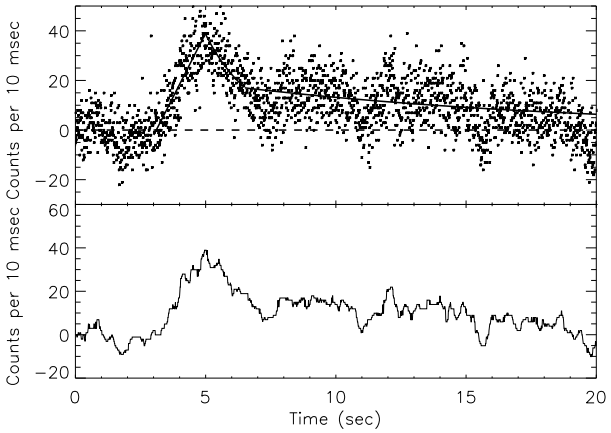

Fig. 6. OPTIMA light curve of flare 1 at a time resolution of 10 ms (*top panel*) together with an empirical fit (see text for details) and median averaged light curve (*bottom panel*).

In summary, we can state that on time scales of 10 ms our OPTIMA light curves of UV Cet show some small degree (about 5%) of autocorrelation, which we attribute to scintillation effects. In time bins of 10 ms we typically find about 40 source count (cf., Fig. 3.) out of which 1−2 are unrelated to the source. The observed count distributions resemble Poisson distributions with some extra noise. The background channels show no signatures of auto- or crosscorrelation effects as expected.

In the following we concentrate on the source channel and specifically on the two flares observed in the night of Oct. 7th 2008 (see Fig. 3). The brighter flare (henceforth Flare 1) occurred at 9370 s while the fainter peak (Flare 2) happened at 6450 s. No flares were detected in the observations from Oct. 6th 2008.

3.3. Flare 1

In Fig. 6 (lower panel) we show an excerpt of our UV Cet light curve at a time resolution of 10 ms. In order to take out trends and short term oscillations we take chunks of typically 50−100 s of data prior to and after the flare and fit a polynomial of order of up to ten to these data. We then use the fitted polynomial to rectify the OPTIMA data. In order to reduce the noise in the visualisation of the light curves we also apply a sliding median averaging over 250 ms and show the thus obtained smoothed light curve in the bottom panel of Fig. 6, where the typical signature of a flare becomes very much apparent. Additionally, we show an adhoc model fit to the data consisting of a linear rise phase, followed by two exponential decay phases. This is meant only as an empirical description of the data to specify peak flux, fluence and decay time scales of this event; in Table 1 we provide these basic parameters of the flare.

Flare 1 looks like a textbook example of a stellar flare rising steeply to reach its peak within two seconds. The peak lasts only a very short time, at most 1−2 s, afterwards the flux enhancement decreases initially very fast with an estimated decay time scale of about two seconds. A definite break is apparent in the light curve and a much slower decay on a time scale of about 15 s follows. Since it is difficult to determine the zero level with very high precision, this latter time scale and hence the total flux in this slow decay part are therefore less well determined.

Table 1. Measured quantities and derived physical parameters for the two flares observed; see text for details.

Parameter	Flare 1	Flare 2
Peak count rate (s^{-1})	4000	2000
Rise time (s)	≈2	≈1.5
Fast decay time (s)	≈2	≈1.5
Slow decay time (s)	≈13	n.a.
Counts in rise	≈4000	≈1600
Counts in fast decay	≈3900	≈3800
Counts in slow decay	≈600	n.a.
Quiescent rate (cts/s)	3700	3700
Peak luminosity (erg/s)	1.6×10^{28}	7.9×10^{27}
Energy (rise, erg)	1.6×10^{28}	6.3×10^{27}
Energy (decay fast)	1.5×10^{28}	1.5×10^{28}
Energy (decay slow)	2.4×10^{27}	n.a.
Energy (total)	3.3×10^{28}	2.1×10^{28}
Area (cm^2)	2×10^{16}	1.4×10^{16}

The flare light curve exhibits multiple flux drops with a quasi-regular spacing of about four seconds. This pattern is only detected during the flare and not in the non-flaring UV Cet light curve data. No such behavior has been seen in any other source observed with OPTIMA and no potential instrumental features appearing with that period are known. Thus, the probability is high that the observed quasi periodicity is source intrinsic. Experimental verification of such oscillations in other flares is certainly highly desirable.

3.4. Flare 2

Flare 2 was analyzed with the same procedures as for flare 1. The resulting light curve (shown in Fig. 7) shows that the morphology of flare 2 is very similar to that of flare 1. However, flare 2 is less bright and thus the slow decay section of the light curve is not readily apparent in the unbinned data. The median averaged light curve does suggest an enhanced level lasting for about eight seconds. The resulting fit parameters for flare 2 are also included in Table 1.

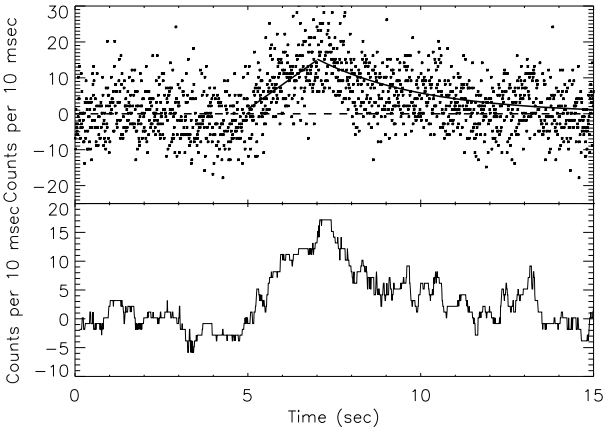

Fig. 7. OPTIMA light curve of flare 2 at a time resolution of 10 ms (*top panel*) together with an empirical fit (see text for details) and median averaged light curve (*bottom panel*).

3.5. Comparison to MANIA observations

The flare patrol time of our OPTIMA UV Cet observations was considerably shorter than the >35 h patrol time reported by Beskin et al. (1988) for MANIA. In addition, the large majority of the MANIA observations were obtained with the *U*-band filter and only a few were taken in the *B*-band, similar to our passband. Unsurprisingly, Beskin et al. (1988) thus reported 118 *U*-band, but only 4 *B*-band flares. As no detailed analysis of all observed MANIA flares is available, we can only state that some of their flares very much resemble the two events observed with OPTIMA.

3.6. Energetics

In the following section we provide a rough estimate of the energetics of the two flares observed with OPTIMA. In this context we note again that the blue filter used for our OPTIMA observations is not a standard filter, however, we assume for simplicity that the filter response is that of a Johnson *B* filter. This assumption should not be crucial since we cannot determine the temperature of the flare plasma from our single band observations anyway, and therefore the overall energetics can be determined only very approximately. For the purposes of our discussion we assume a bolometric magnitude of both components of UV Cet of 11.77 (Greenstein 1989), which corresponds to a bolometric luminosity at UV Cet's distance of $L_{\rm bol} \approx 6.8 \times 10^{30}$ erg s^{-1}. Furthermore we assume that an apparent magnitude of $m_{\rm b} = 0$ corresponds to an energy flux outside the Earth's atmosphere of 6.49×10^{-6} erg cm^{-2} s^{-1}. Using these numbers as well as an apparent *B* magnitude of 13.86 we compute an energy flux (in the blue band) of 1.85×10^{-11} erg cm^{-2} s^{-1} and a total blue luminosity of 1.5×10^{28} erg s^{-1} for the UV Cet binary system.

To determine the quiescent source photon flux, we determine the median dark SPAD count rate from the exposure with closed shutter, estimate the sky background from the fibers surrounding the target fiber and correct for individual fiber efficiencies. As the SPAD counts in the central fiber are dominated by source counts, these corrections are quite small. Associating the observed quiescent photon flux observed before and after the flares with an energy flux of 1.85×10^{11} erg cm^{-2} s^{-1} results in a luminosity to count rate conversion factor of 3.95×10^{24} erg/count for our OPTIMA UV Cet data. Assuming then that this conversion factor is the same also for the flare data, we can assess the peak luminosity in the blue band (in terms of erg/s) and the total emitted *B* band energy.

As the temperature of the flare plasma is bound to change with respect to quiescent conditions, our energy conversion can naturally only be approximately correct. We note that while under quiescent conditions the blue luminosity accounts for only a small fraction of the overall energy losses, the flaring regions have considerably higher luminosities. Thus, the blue band should actually capture a substantial fraction of the overall optical energy losses. Needless to say, no statements about energy losses in other than the observed band can be made, thus our estimates should be considered as lower limits.

Taking the observed values as given in Table 1, we can derive the energetics of the observed flare events. Here we concentrate on the rise and rapid decay phase, as the slow decay phase is difficult to discriminate for the weaker flare and the time scale and hence the total fluence are poorly constrained. As data were only obtained with a single filter the temperature of the flaring plasma cannot be determined. However, from other flare observations we know that typical temperatures are on the order of 10 000 K. With such temperatures any bolometric corrections ought to be small. Therefore the derived numbers should be representative for the whole energy emitted in the optical regime. Naturally we cannot make any statements on energy losses in other wavebands, which are likely to occur and thus our numbers should be considered as lower limits.

From the determined peak luminosity we then derive a characteristic area of 1–2 $\times 10^{16}$ cm^2 as the emitting surface on the star, assuming a canonical effective temperature of 10 000 K. While clearly these estimates should be considered only as order of magnitude estimates that depend sensitively on temperature, it is clear that the characteristic size of the flaring regions is quite small with an extent of less than one thousand kilometers.

4. Discussion and conclusions

The peak luminosities of the flares recorded in our OPTIMA observations reach about 50−100% of the star's quiescent *B*-band luminosity. Their total energy output equals that emitted by the star in a few seconds in the *B*-band, yet they clearly make only very small contributions to the overall energy output of the star, given its bolometric luminosity of 6×10^{30} erg s^{-1}. The recorded fluctuations make a reliable identification of shorter lasting or weaker flares difficult. We are, however, confident that in the total OPTIMA patrol time on UV Cet (a total of less than five hours) no stronger flares than the above reported flares 1 and 2 occurred.

With our overall, rather short patrol time on UV Cet we can state that the average *B*-band energy input is on the order of 3–4 $\times 10^{24}$ erg s^{-1} with significant uncertainties. This number is two orders of magnitude smaller than the *U*-band value as quoted by Doyle & Butler (1985).

Lacy et al. (1976) studied the overall energetics of flares observed on different stars in different energy bands and found the relation $E_U = (1.2 \pm 0.08) E_B$ over several orders of magnitude. Using this relation suggests that our *B*-band flare "survey" is highly incomplete and misses substantial numbers of small flares. Observations in the *U*-band should reduce photospheric "background" by a factor of about 3 or more and correspondingly increase our sensitivity to detect even smaller flares. The energetics derived in the *B*-band puts the flares – not surprisingly – at the low end of the observed flare energetics distribution derived by Lacy et al. (1976) for UV Cet.

The rise times of the observed flares were on the order of two seconds. Shvartsman et al. (1988) report the rise times of 10 flares observed on UV Cet, two of those had rise times comparable to or even shorter than the rise times reported for flares 1 and 2. Thus, the observed rise times are short, yet not unusually so. It is not clear whether the observed rise times should be color dependent. High spectral resolution observations of a giant flare on CN Leo suggest a markedly different behavior of the flaring plasma during the impulse and gradual phase (Fuhrmeister et al. 2008). However, this giant flare on CN Leo may not be comparable to the by comparison rather tiny flares discussed here.

There are various reports about apparent flux oscillations for active late type dwarf stars. A still prominent example is a long duration flare on the Hyades star H II 2411 observed by Rodono (1974), showing coherent oscillations with a period of 13 s throughout its eruption. Further, Zhilyaev et al. (2000) report the results on multi-site, multi-band observations of the flare star EV Lac, finding "coherent" oscillations in three out of 19 recorded flares with periods in the range 13 s and 26 s on rather long duration flares lasting more than 100 s. Unfortunately these authors do not discuss flares with shorter durations, although the time resolution of their data (0.1 s) would have allowed them to do so. At any rate, if we accept the observed oscillations in flare 1 as real and associate the observed period τ with the size and Alfven speed through $\tau = L/v_A$, we find – using $L \sim 10^8$ cm, $B \sim 10^3$ G and $\tau \sim 4$ s densities $n \sim 10^{14}$ cm^{-3}, which fit to the expected chromospheric origin of the flare radiation.

It is instructive to compare the energetics derived for the optical flares to the X-ray data for UV Cet. UV Cet's quiescent flux in the soft X-ray band is typically on the order of 2–3 $\times$ 10^{27} erg s^{-1}, and for comparison, the potentially weakest X-ray flare from UV Cet reported to date (Schmitt et al. 1993) had a total emitted energy of 1.5×10^{29} erg, i.e. on the same order of the total energy loss of the optical flares reported in this paper.

Heating by so-called "microflares" and "nanoflares" (Cargill & Klimchuk 2004; Klimchuk 2006) is a popular hypothesis to explain the heating of the corona of the Sun and that of other stars. Their nanoflare model assumes that any coronal loop is composed of many unresolved strands of magnetic flux and that these strands are "heated impulsively by a small burst of energy, which, for convenience, are called a nanoflare, although the range of energies is completely arbitrary". However, the energies of the flare events observed on UV Cet are still orders of magnitude above the nanoflare energetics discussed in the context of heating the solar corona. At any rate, it would be interesting to explore a possible connection of optical microflaring to analogous X-ray activity in a more systematic way, and we therefore encourage co-temporaneous X-ray and optical observations with a high time resolution.

In summary, OPTIMA is well suited for the study of rapid variability on late-type stars. Clearly, the usage of a bluer filter (e.g., U-band) together with SPADs with enhanced quantum efficiency at lower wavelengths would greatly enhance our ability to detect events of even lower luminosities at shorter wavelengths. Our (currently) sparse observational material confirms previous findings of the MANIAC team that the typical time scale for stellar flares (in the optical) can be in the range 0.1−1 s, although most flares have – just like "our" flares on UV Cet – overall durations in excess of 1 s. Therefore time resolutions in the range 1−10 ms are sufficient for a full description of the relevant phenomena. We finally note high spectral resolution observations of flare events with possibly sub-second cadence might provide a science case for very large telescopes. We expect the occurrence of spectral changes both in the form of temperature changes as well as in the appearance and disappearance of emission lines on short time scales and a theoretical modelling of such processes, requiring a combined treatment of hydrodynamics and radiative transfer, is now within reach of numerical astrophysics.

Acknowledgements. This research has made use of the SIMBAD database, operated at CDS, Strasbourg, France. Skinakas Observatory is a collaborative project of the University of Crete (UoC) and the Foundation for Research and Technology Hellas (FORTH), and the Max-Planck-Institute for Extraterrestrial Physics. This work was in part supported under the FP7 Opticon European Network for High Time Resolution Astrophysics (HTRA) project. We want acknowledge the contributions of Natalia Lewandowska (UHH) and Natalia Primak (IfA), who participated in the observing campaigns yielding the data analyzed in this paper.

References

Audard, M., Güdel, M., & Skinner, S. L. 2003, ApJ, 589, 983
Beskin, G. M., Neizvestnyi, S. I., Pimonov, A. A., Plakhotnichenko, V. L., & Shvartsman, V. F. 1982, IAU Colloq. 67: Instrumentation for Astronomy with Large Optical Telescopes, 92, 181
Beskin, G. M., Chekh, S. A., Gershberg, R. E., et al. 1988, Sov. Astron. Lett., 14, 65
Betta, B., Peres, G., Reale, F., & Serio, S. 1997, A&AS, 122, 585
Brown, J. C. 1973, Sol. Phys., 28, 151
Cargill, P. J., & Klimchuk, J. A. 2004, ApJ, 605, 911
Dravins, D., Lindegren, L., Mezey, E., & Young, A. T. 1997, PASP, 109, 173
Doyle, J. G., & Butler, C. J. 1985, Nature, 313, 378
Fuhrmeister, B., Liefke, C., Schmitt, J. H. M. M., & Reiners, A. 2008, A&A, 487, 293
Geyer, D. W., Harrington, R. S., & Worley, C. E. 1988, AJ, 95, 1841
Greenstein, J. L. 1989, PASP, 101, 787
Jackson, P. D., Kundu, M. R., & White, S. M. 1989, A&A, 210, 284
Kanbach, G., Stefanescu, A., Duscha, S., et al. 2008, Astrophys. Space Sci. Libr., 351, 153
Klimchuk, J. A. 2006, Sol. Phys., 234, 41
Kürster, M., & Schmitt, J. H. M. M. 1996, A&A, 311, 211
Lacy, C. H., Moffett, T. J., & Evans, D. S. 1976, ApJS, 30, 85
Neupert, W. M. 1968, ApJ, 153, L59
Moffett, T. J. 1972, Nat. Phys. Sci., 240, 41
Parker, E. N. 1988, ApJ, 330, 474
Peres, G. 2000, Sol. Phys., 193, 33
Robinson, R. D., Carpenter, K. G., Percival, J. W., & Bookbinder, J. A. 1995, ApJ, 451, 795
Rodono, M. 1974, A&A, 32, 337
Sánchez Almeida, J. 2001, ApJ, 556, 928
Schmitt, J. H. M. M., Haisch, B. M., & Barwig, H. 1993, ApJ, 419, L81
Shvartsman, V. F., Beskin, G. M., Gershberg, R. E., Plakhotnichenko, V. L., & Pustilnik, L. A. 1988, Sov. Astron. Lett., 14, 97
Syratovskii, S. I., & Shmeleva, O. P. 1972, Sov. Astron., 16, 273
Tovmassian, H. M., Recillas, E., Cardona, O., & Zalinian, V. P. 1997, Rev. Mex. Astron. Astrofis., 33, 107
Vilmer, N., Trottet, G., Barat, C., et al. 1994, Space Sci. Rev., 68, 233
Zhilyaev, B. E., Verlyuk, I. A., Romanyuk, Y. O., et al. 1998, A&A, 334, 931
Zhilyaev, B. E., Romanyuk, Y. O., Verlyuk, I. A., et al. 2000, A&A, 364, 641